

Evolutionary calculations of carbon dredge-up in helium envelope white dwarfs

James MacDonald¹, Margarita Hernanz² and Jordi José³

¹ *Department of Physics and Astronomy, University of Delaware, Newark, DE 19716*

² *Institut d'Estudis Espacials de Catalunya, CSIC Research Unit, Edifici Nexus-104, C/Gran Capità, 2-4, E-08034 Barcelona, SPAIN*

³ *Departament de Física i Enginyeria Nuclear (UPC), Avda. Victor Balaguer, s/n, E-08800 Vilanova i la Geltru, SPAIN*

Accepted ???? . Received 1997 ; in original form 1997

ABSTRACT

We investigate the evolution of cooling helium atmosphere white dwarfs using a full evolutionary code, specifically developed for following the effects of element diffusion and gravitational settling on white dwarf cooling. The major difference between this work and previous work is that we use more recent opacity data from the OPAL project. Since, in general, these opacities are higher than those available ten years ago, at a given effective temperature, convection zones go deeper than in models with older opacity data. Thus convective dredge-up of observationally detectable carbon in helium atmosphere white dwarfs can occur for thicker helium layers than found by Pelletier et al (1986). We find that the range of observed C to He ratios in different DQ white dwarfs of similar effective temperature is well explained by a range of initial helium layer mass between 10^{-3} and $10^{-2}M_{\odot}$, in good agreement with stellar evolution theory, assuming a typical white dwarf mass of $0.6M_{\odot}$. We also predict that oxygen will be present in DQ white dwarf atmospheres in detectable amounts if the helium layer mass is near the lower limit compatible with stellar evolution theory. Determination of the oxygen abundance has the potential of providing information on the profile of oxygen in the core and hence on the important $^{12}\text{C}(\alpha, \gamma)^{16}\text{O}$ reaction rate.

Key words: diffusion – stars: abundances – stars: interiors – stars: white dwarfs

1 INTRODUCTION

DQ white dwarfs have He-rich atmospheres, with the presence of a trace of carbon. The results of model atmosphere calculations for 24 DQ white dwarfs have been compiled by Weidemann & Koester (1995). Effective temperatures, T_{eff} , range from 12,500 K to 6,700 K. $\log(n(\text{C})/n(\text{He}))$ values determined from visual spectra range from -6.2 to -1.5 . Analysis of IUE spectra have pushed the lower limit to -7.3 . The generally accepted explanation for the presence of trace carbon in these cool He white dwarf atmospheres is that carbon from the core diffuses outwards to where convection dredges it to the surface. The first detailed calculations of this process were presented by Pelletier et al. (1986) (hereafter P86), who show how, in the hotter phases, carbon diffuses upwards from the core to be met eventually by the base of the surface convection zone that develops due to the increase in opacity following recombination of helium as the white dwarf cools. With further cooling more carbon diffuses upwards and the base of convection zone moves deeper into the star, further enriching the outer layers with carbon. A key finding of this research is that the maximum depth of the base of the convection zone nearly coincides with a change in ionization state of the carbon below the convection zone. Since the slope of the carbon profile depends on

the relative ionization states of carbon and helium, this reduction in ionization state of carbon results in a steepening profile and a reduction in the carbon abundance in the convection zone. It is this change in ionization structure that causes a reduction in observed $n(\text{C})/n(\text{He})$ values at lower temperatures, and the non-detection of carbon below 6,000 K. Since the thickness of the helium layer regulates the effective temperature at which the base of the convection zone reaches regions of diffusively enhanced carbon, the observations of DQ white dwarfs place limits on the amount of helium in the white dwarf, that can be compared to the predictions of stellar evolution theory. P86 concluded that models for a white dwarf mass of $M_{*} = 0.6M_{\odot}$ and a helium envelope mass, M_{env} , in the range 10^{-4} to $10^{-3.5}M_{*}$ gave the best fit to the contemporary observational data. This is in conflict with evolutionary models for post AGB stars that predict that M_{env} should be in the range 10^{-3} to $10^{-2}M_{\odot}$ for this core mass. To complicate the picture further, models of the non-radial g-mode pulsations of the DBV star GD 358 fit the observations best for $M_{*} = 0.61M_{\odot}$ and $M_{\text{env}} = 10^{-5.7 \pm 0.3}M_{*}$ (Winget et al. 1994, Bradley & Winget 1994), which is significantly less than both the estimates from the DQ white dwarf models of P86 and post AGB evolution models.

In this paper, we have reinvestigated the evolution of

cooling helium atmosphere white dwarfs for a range of M_* and M_{env} , using a full evolutionary code, specifically developed for following the effects of element diffusion and gravitational settling on white dwarf cooling. The major difference between this work and that of P86 is that here we use the more recent opacity data from the OPAL project (Iglesias & Rogers 1993). Since, in general, these opacities are higher than those available ten years ago, at a given effective temperature, convection zones go deeper than in models with older opacity data. Thus convective dredge-up of observationally detectable carbon in helium atmosphere white dwarfs can occur for thicker helium layers than found by P86. We find that the range of observed C to He ratios in different DQ white dwarfs of similar effective temperature is well explained by a range of M_{env} between 10^{-3} and $10^{-2}M_{\odot}$, in good agreement with stellar evolution theory, assuming a typical white dwarf mass of $0.6M_{\odot}$.

The details of the evolutionary code are given in the next section. In section 3, we present our results for the evolution of the abundance profiles and compare them with observations and current ideas for the evolution of possible white dwarf progenitors. Our conclusions are given in section 4.

2 MODELING DIFFUSION AND CONVECTIVE MIXING IN COOLING WHITE DWARFS

To study the evolution of the carbon distribution in helium atmosphere white dwarfs, we have added routines that solve the equations describing element diffusion and gravitational settling to a stellar evolution code specifically designed for following the cooling history of white dwarfs. We restrict attention to mixtures of helium, carbon and oxygen. The existence of OPAL opacities for arbitrary mixtures of these three elements allows us to calculate consistently the effects of element diffusion on the optical thickness of the non-degenerate envelope, which controls the rate of cooling of the white dwarf. These effects were not included by P86. The initial model consists of a core of uniform composition, surrounded by an envelope also of uniform composition. The initial temperature profile is determined by computing a thermal equilibrium model, in which radiative and neutrino losses are balanced by an artificial constant energy rate, ε_c . We study three sets of models, labeled HE, LO, and PG. To identify our sequences, we use an alphanumeric label that consists of three parts. The first part identifies the core mass, the second part the particular set of models to which the sequence belongs, and the third part identifies the envelope mass. For example, the P6HE6 sequence is part of the HE set of models and has a core mass of $0.6M_{\odot}$ and envelope mass of approximately $10^{-6}M_{\odot}$. The HE set is the largest set of models and explores how the degree of carbon and oxygen dredge-up depends on core mass and envelope mass. The LO set has a lower core oxygen abundance than the HE set and is used to explore the relation between the oxygen abundance in DQ photospheres and the oxygen abundance in the core. The PG sequence has envelope composition characteristic of the PG1159 stars and is used to test the idea that some DQ white dwarfs are descendants of the PG1159 stars. In particular, Dehner & Kawaler (1995) have suggested that the unusual DBQv GD 358 is such an

object. The properties of our initial models are given in Table 1. M_{core} , $X_{\text{C,core}}$, $X_{\text{O,core}}$ and M_{env} , $X_{\text{C,env}}$, $X_{\text{O,env}}$ are the initial masses, carbon mass fraction and oxygen mass fraction of the CO core and He-rich envelope respectively. Our range of M_{env} values at $0.6M_{\odot}$ was chosen to include those from the asteroseismological studies of GD 358 up to the largest values consistent with stellar evolution models for the white dwarf progenitor.

We stop our evolutionary calculations when the temperature at zero optical depth is 6,000 K, which is the lowest temperature in the OPAL opacity tables. This corresponds to $T_{\text{eff}} = 7,000$ K.

The treatment of diffusion is fairly straightforward. We use an approach that is applicable to a general mixture of an arbitrary number of elements. We neglect thermal diffusion, which has been shown to be negligible for white dwarfs by Iben & MacDonald (1985), and Paquette et al. (1986b) and radiative levitation. Although radiative levitation is important for determining the photospheric composition of hot white dwarfs (Fontaine & Michaud 1979, Vauclair, Vauclair & Greenstein 1979), it is entirely negligible in the interior and also in the photospheric regions at the effective temperatures of the DQ white dwarfs. For simplicity, we also neglect magnetic fields and stellar rotation. The composition profiles are then determined by the competition between gravity, partial pressure gradients and induced electric fields. The diffusion velocities satisfy (Curtiss & Hirschfelder 1949, Aller & Chapman 1960, Burgers 1969, Muchmore 1984, Iben & MacDonald 1985) the multi-fluid equations

$$\frac{dp_i}{dr} - \frac{\rho_i}{\rho} \frac{d\rho}{dr} - n_i Z_i e E = \sum_j K_{ij} (w_j - w_i) \quad (1)$$

where p_i , ρ_i , n_i , Z_i , w_i are the partial pressure, mass density, number density, mean charge, and diffusion velocity for species i and E is the electric field induced by the gradients in the ion densities. The resistance coefficients are from Paquette et al (1986a).

In solving equations (1) for the diffusion velocities, care must be taken to avoid rounding errors due to the subtractions. This is particularly important for the diffusion velocities of trace elements. For N species including electrons, equations (1) is a set of $N - 1$ independent linear equations for $N + 1$ unknown variables (the w_i 's and E). To complete the set of equations, we use the conditions for no net mass flow relative to the center of mass

$$\sum_i A_i n_i w_i = 0 \quad (2)$$

and charge neutrality

$$\sum_i Z_i n_i = 0 \quad (3)$$

In equations (2) and (3), the sums are over all species (ions, neutrals and electrons). We assume the electron to have zero mass. The electrical field can then be eliminated directly since equation (1) applied to electrons gives

$$E = - \frac{1}{en_e} \frac{dp_e}{dr} \quad (4)$$

The electron pressure, p_e , and the electron number density, n_e , can now be eliminated since

$$p_e = p - \sum_{i \neq e} p_i \quad (5)$$

and

$$n_e = \sum_{i \neq e} Z_i n_i \quad (6)$$

where the sums now do not include the electrons. Using the equation of hydrostatic balance, equation (1) can be transformed to

$$\begin{aligned} \frac{dp_i}{dp} - X_i + \frac{n_i Z_i}{\sum_{j \neq e} n_j Z_j} \left[1 - \sum_{j \neq e} \frac{dp_j}{dp} \right] = \\ - \sum_{j \neq e} \frac{K_{ij}}{\rho g} (w_j - w_i) \end{aligned} \quad (7)$$

To reduce rounding errors, we reformulate equation (7) as

$$\begin{aligned} \left(\frac{dp_i}{dp} - X_i \right) \frac{\sum_{j \neq i, j \neq e} \frac{X_j Z_j}{A_j}}{\sum_{j \neq e} \frac{X_j Z_j}{A_j}} - \frac{X_i Z_i}{A_i} \frac{\sum_{j \neq i, j \neq e} \left(\frac{dp_j}{dp} - X_j \right)}{\sum_{j \neq e} \frac{X_j Z_j}{A_j}} = \\ - \sum_{j \neq e} \frac{K_{ij}}{\rho g} (w_j - w_i) \end{aligned} \quad (8)$$

The equations for the changes in mass fractions due to element diffusion and convective mixing are

$$\frac{dX_i}{dt} + \frac{\partial F_i}{\partial m} = 0 \quad (9)$$

where the fluxes, F_i , are

$$F_i = 4\pi r^2 \rho w_i X_i + \sigma_{\text{con}} \frac{\partial X_i}{\partial m} \quad (10)$$

Convective mixing is treated as a diffusion process, with diffusion coefficient, $\sigma_{\text{con}} = (4\pi r^2 \rho l)^2 / \tau_{\text{con}}$ where l is the mixing length and τ_{con} is the convective turnover time scale calculated from mixing length theory.

Equations (9) and (10) for each element are solved together with the equations of stellar structure by standard implicit finite difference techniques. The diffusion velocities, w_i , are first found by standard matrix methods (LU decomposition), from finite difference equations derived from equations (8).

This multi-fluid formulation requires knowledge of the partial pressures, p_i . For non-interacting species or species interacting through short-range forces such as Van der Waals forces, calculation of p_i is relatively straightforward. However for species interacting through long-range coulomb forces, it is not clear that the concept of partial pressures is meaningful. We circumvent this difficulty by adopting a ‘linear mixing law’,

$$p_i = n_i \frac{\sum_{j \neq e} p_j}{\sum_{j \neq e} n_j} \quad (11)$$

3 EVOLUTION OF THE ABUNDANCE PROFILES

Figure 1 shows how the carbon mass fraction changes with T_{eff} for the P6HE3 sequence. Also shown are the location of the photosphere and the boundaries of the convection zones. This figure can be compared to figure 1 of P86. The most important difference is in M_{cmax} , the maximum depth of the inner boundary of the convection zone. For $M_* = 0.6M_\odot$, and $M_{\text{env}} = 1.9 \cdot 10^{-4} M_\odot$, P86 find $M_{\text{cmax}} = 3.8 \cdot 10^{-7} M_\odot$, which occurs when T_{eff} is near 10^4 K. For the P6HE4 and P6HE3 sequences, we find $M_{\text{cmax}} = 1.8 \cdot 10^{-6}$ and $1.7 \cdot 10^{-5} M_\odot$, respectively. We attribute most of the order of magnitude difference in M_{cmax} to differences in radiative opacity. Although the depth of the convection zone is sensitive to convective efficiency for relatively high effective temperatures, Fontaine, Tassoul & Wesemael (1984) have shown that at temperatures characteristic of DQs the dependence is significantly less. To illustrate this, we have calculated cooling sequences without element diffusion for a $0.61M_\odot$ white dwarf with $M_{\text{env}} = 10^{-2} M_\odot$ and mixing length ratios, $\alpha = 1.0, 1.5$ and 2.0 . In figure 2, we show the location of the convection zone inner boundary for pure helium envelopes and envelopes that are a mixture of helium and carbon with $X_C = 10^{-3}$. To test the dependence of M_{cmax} on opacity, we have also calculated cooling sequences using the Los Alamos opacities (Huebner et al. 1977). In figure 3, we show the location of the convection zone inner boundary for the helium and carbon mixture for the OPAL and Los Alamos opacities. It is clear that the newer opacities result in deeper convection zones and that the depth of the convection zone is insensitive to α for $T_{\text{eff}} < 14,000$ K. We also see that the presence of carbon in small amounts reduces the depth of the convection zone, and hence the convection zone in the P6HE4 sequence is smaller than that of the P6HE3 sequence.

3.1 Comparison with observations and prior evolution

In figure 4, we show the ratio of the number densities of carbon and helium in the convection zone as a function of T_{eff} for the models with $M_{\text{core}} = 0.6M_\odot$. Also shown are the observed photospheric ratios taken from Weidemann & Koester (1995). When possible, error bars are from the individual papers referenced in Weidemann & Koester (1995). Excluding the stars for which there are only upper limits, the mean of the observed C to He ratios is $\log n(\text{C})/n(\text{He}) = -5.35$ and the corresponding mean T_{eff} is 9,300 K. For our models with $M_{\text{core}} = 0.6M_\odot$, these values are obtained if $M_{\text{env}} = 1.1 \cdot 10^{-2} M_\odot$.

There are many possible ways that helium atmosphere white dwarfs can form. They may be descendants of asymptotic giant branch (AGB) stars or sdOs. They may also be the result of mergers in double degenerate systems. Because the evolutionary state of sdO stars is poorly understood and the physics of mergers is very complex, we assume here that

Table 1. Properties of the initial models

| Sequence | M_{core} | $X_{\text{C,core}}$ | $X_{\text{O,core}}$ | M_{env} | $X_{\text{C,env}}$ | $X_{\text{O,env}}$ | R | T_{eff} | ρ_c | T_c |
|----------|-------------------|---------------------|---------------------|-----------------------|--------------------|--------------------|-------|------------------|----------|-------|
| P6HE6 | 0.600 | 0.50 | 0.50 | 4.93×10^{-7} | 0.01 | 0.01 | 1.13 | 7.45 | 2.78 | 1.07 |
| P6HE4 | 0.600 | 0.50 | 0.50 | 9.36×10^{-5} | 0.01 | 0.01 | 1.16 | 7.40 | 2.78 | 1.07 |
| P6HE3 | 0.600 | 0.50 | 0.50 | 9.60×10^{-4} | 0.01 | 0.01 | 1.14 | 7.45 | 2.80 | 1.07 |
| P6HE2 | 0.602 | 0.50 | 0.50 | 8.29×10^{-3} | 0.01 | 0.01 | 1.13 | 7.43 | 2.97 | 1.06 |
| P6LO3 | 0.600 | 0.99 | 0.01 | 1.02×10^{-3} | 0.01 | 0.01 | 1.16 | 7.49 | 2.69 | 1.03 |
| P6LO2 | 0.602 | 0.99 | 0.01 | 8.29×10^{-3} | 0.01 | 0.01 | 1.15 | 7.47 | 2.86 | 1.07 |
| P6PG6 | 0.600 | 0.50 | 0.50 | 4.41×10^{-6} | 0.50 | 0.17 | 1.88 | 10.97 | 1.40 | 2.02 |
| 1HE4 | 1.00 | 0.50 | 0.50 | 1.01×10^{-4} | 0.01 | 0.01 | 0.590 | 7.68 | 30.7 | 1.08 |
| 1HE3 | 1.00 | 0.50 | 0.50 | 1.02×10^{-3} | 0.01 | 0.01 | 0.590 | 7.73 | 30.9 | 1.10 |

Units are M_{\odot} for masses, 10^9 cm for R , 10^4 K for T_{eff} , 10^6 g cm $^{-3}$ for ρ_c , and 10^8 K for T_c .

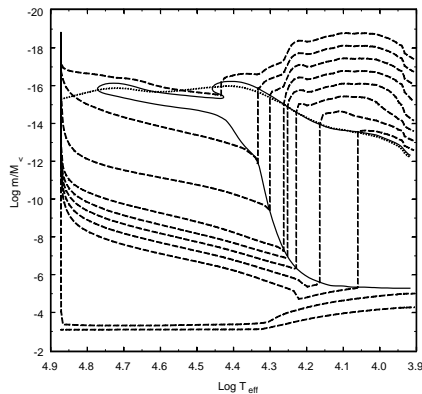


Figure 1. Convection zone boundaries (solid line), location of the photosphere (dotted line) and contours of carbon mass fraction (dashed lines) for the P6HE3 sequence. The contour levels are, from top to bottom, $\log X_{\text{C}12} = -10, -9, \dots, -1$.

DQs have AGB predecessors.

The possible modes of how AGB stars evolve to white dwarfs have been described in detail by Iben (1984). In contrast to the case for DA white dwarfs, there have been too few detailed calculations of the evolution to helium atmosphere white dwarfs for us to be precise about the mass of helium in these objects. However due to the relationship between the white dwarf and its AGB predecessor, we find it convenient to parameterize M_{env} in terms of $M_{\text{He}}^{\text{init}}$, the mass of the helium layer just prior to ignition of a helium shell flash. This is given by (Iben & Tutukov 1996)

$$\log M_{\text{He}}^{\text{init}} = -1.835 + 1.73M_{\text{core}} - 2.67M_{\text{core}}^2 \quad (12)$$

for $M_{\text{core}} \geq 0.55M_{\odot}$. This is in good agreement with the results for the final helium layer mass from unpublished calculations by one of us (JM) of the evolution of population I helium stars of masses between 0.5 and $0.8 M_{\odot}$ to the white dwarf stage. For less massive cores, we find that this equation underestimates $M_{\text{He}}^{\text{init}}$.

Whether the final white dwarf has a hydrogen-deficient envelope or not depends on the phase of the thermal pulse cycle at which the star leaves the AGB. If this occurs during helium shell burning, winds can remove all remaining

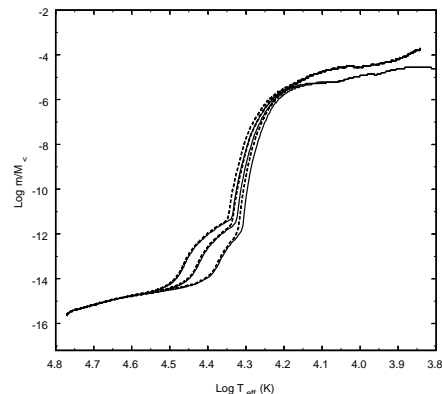


Figure 2. Location of the inner boundary of the convection zone for a $0.61M_{\odot}$ white dwarf with $M_{\text{env}} = 10^{-2}M_{\odot}$ and mixing length ratios, $\alpha = 1.0, 1.5$ and 2.0 (from bottom to top). The solid lines are for $X_{\text{C}} = 10^{-3}$ and the dashed lines are for $X_{\text{C}} = 0$.

hydrogen. Thus we might expect M_{env} to be close to $M_{\text{He}}^{\text{end}}$, the mass of the helium layer at the end of quiescent helium burning, in a star that is near the tip of the AGB (D'Antona & Mazzitelli 1991). This is about 30% of $M_{\text{He}}^{\text{init}}$ (Vassiliadis & Wood 1993; Iben & Tutukov 1996). D'Antona & Mazzitelli (1991) estimate that M_{env} will be about 30% less than $M_{\text{He}}^{\text{end}}$ because carbon and other heavy elements will sink out of the helium buffer layer as the star evolves to a white dwarf. However, Iben & Tutukov (1984) find for $M_{*} = 0.6M_{\odot}$, that $M_{\text{env}} = 0.016M_{\odot}$, which is about $0.9 M_{\text{He}}^{\text{init}}$. Thus $M_{\text{env}}/M_{\text{He}}^{\text{init}}$ is of order 0.2 to 1.0 so that for $M_{\text{core}} = 0.6M_{\odot}$, we estimate M_{env} is between $3.5 \cdot 10^{-3}$ and $1.7 \cdot 10^{-2}M_{\odot}$, which is in reasonably agreement with the mean value derived above for the DQ white dwarfs. Furthermore this range of M_{env} corresponds to a range in $\log n(\text{C})/n(\text{He})$ at 9,300 K of -4.2 to -5.8 . Although many of the DQs lie within these limits, clearly some of the data points fall outside this range. The DQ white dwarf with the largest C to He ratio, G35-26, has $\log n(\text{C})/n(\text{He}) = -1.5$ and $T_{\text{eff}} \approx 12,500$ K. If $M_{\text{core}} = 0.6M_{\odot}$, this would require $M_{\text{env}} = 2 \cdot 10^{-5}M_{\odot}$. At the other extreme, there are two DZ, two DB and 1 DBA white dwarfs with upper limits to $\log n(\text{C})/n(\text{He})$ of less than -6.5 .

We suggest that DQs with very high C to He ratios are

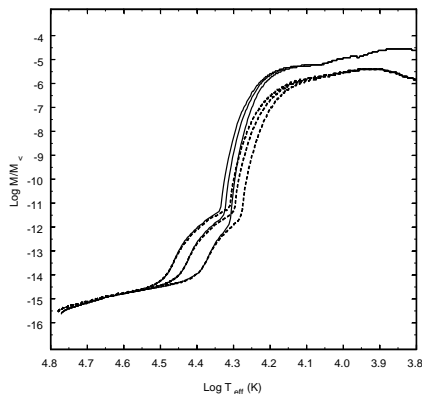


Figure 3. Location of the inner boundary of the convection zone for a $0.61M_{\odot}$ white dwarf with $M_{\text{env}} = 10^{-2}M_{\odot}$ and mixing length ratios, $\alpha = 1.0, 1.5$ and 2.0 (from bottom to top). The solid (dashed) lines are for when OPAL (Los Alamos) opacities are used.

significantly more massive than the typical white dwarf. Due to the higher gravity these have smaller scale heights in the outer layers, which leads to less massive helium envelopes. Figure 5 is the same as figure 4 except that the core mass is $1.0 M_{\odot}$. The solid lines are for envelope masses of 10^{-4} and $10^{-3}M_{\odot}$. The range in M_{env} consistent with prior evolution is $5.0 \cdot 10^{-4} < M_{\text{env}} < 1.7 \cdot 10^{-3}M_{\odot}$. Extrapolating our results at 0.6 and $1.0 M_{\odot}$, we estimate that the minimum core mass consistent with the observed C to He ratio for G35-26 is about $1.3 M_{\odot}$, which is consistent with the high gravity found by Thejll et al. (1990) for this star from analysis of spectra. White dwarfs of mass greater than $1.2 M_{\odot}$, however, are thought to evolve from stars of initial mass between 7.5 and $10 M_{\odot}$ (with an uncertainty of about $0.5 M_{\odot}$ in both limits) which experience quiescent core carbon burning and so develop ONe cores (Domínguez, Tornambé & Isern, 1993; Ritossa, García-Berro & Iben 1996). Hence we can only conclude that the white dwarf in G35-26 is more massive than $1 M_{\odot}$.

Similarly the lowest C to He ratios can be explained by allowing the white dwarf to be less massive than the canonical $0.6 M_{\odot}$. The maximum M_{env} for a $0.5 M_{\odot}$ white dwarf is $0.04 M_{\odot}$. With this much helium, we estimate that $n(\text{C})/n(\text{He}) \sim 10^{-7}$, which is about the lowest detected carbon abundance.

In contrast to P86, we do not find that the carbon abundance starts to drop near $T_{\text{eff}} = 7,000$ K. This difference is due to carbon being fully ionized below the convection zone in the P6HE4, P6HE3 and P6HE2 sequences, whereas P86 find partial recombination. In their calculations, P86 used the Fontaine, Graboske and Van Horn (1977) equation of state. Our equation of state is similar in that it is also based on free energy minimization and is thermodynamically consistent. An important difference that might be the cause of the difference in ionization structure is in the treatment of Stark ionization i.e. the dissolution of bound states due to the ambient electric field from the presence of

free charges. We use the occupancy probability formalism of Hummer and Mihalas (1988). Fontaine et al (1977) divide the temperature- density plane into three regions. In a low density regime, they truncate the partition function by summing over the finite number of bound state energy levels calculated from the static screened coulomb potential. In a high density regime they assume complete ionization. In the intermediate region they interpolate between the low and high density regimes. In table 2, we give some relevant properties of the convection zones for the coolest model of each of the HE sequences. In each case, conditions are such that they lie in the high density fully ionized regime of the Fontaine et al (1977) equation of state. We have already noted that P86 find shallower convection zones. At a mass depth of $4.0 \cdot 10^{-7}M_{\odot}$, corresponding to the depth of the base of the convection zone in the model of P86 with $M_{\text{env}} = 1.9 \cdot 10^{-4}M_{\odot}$, the temperature is $1.7 \cdot 10^6$ K and the density is $7.7 \cdot 10^1 \text{ g cm}^{-3}$ for the P6HE4 model, which again places this point in the high temperature fully ionized region of the Fontaine et al (1977) equation of state. Hence we conclude that the difference in ionization structure in the layers neighboring the base of the convection zone must be due to higher temperatures in our models than those of P86.

3.2 The role of oxygen

The mass fraction of oxygen in the white dwarf core has a strong dependence on the rate of the $^{12}\text{C}(\alpha, \gamma)^{16}\text{O}$ reaction. Although recent experimental progress has reduced the error in this reaction rate to about 35%, this uncertainty can still be significant for nucleosynthesis studies and models of type I supernovae (Arnett 1996). Hence a measurement of the oxygen abundance in the atmosphere of a DQ white dwarf may provide useful information about this reaction rate.

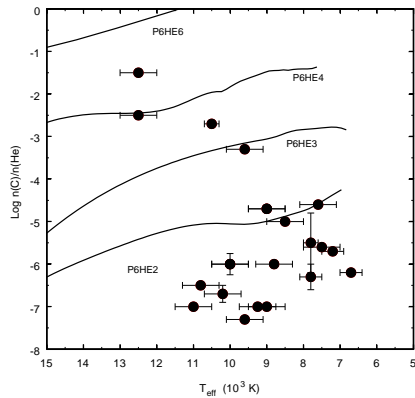
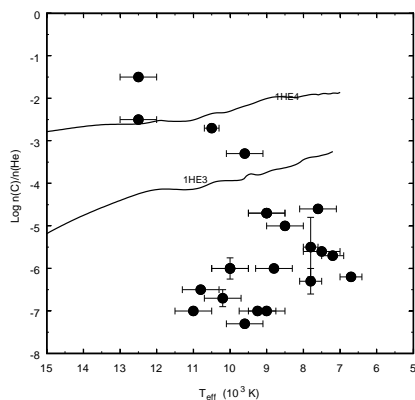
Salaris et al. (1997) have recently calculated the evolution of population I stars of mass 3.2 and $7.0 M_{\odot}$, using the best current estimate for the $^{12}\text{C}(\alpha, \gamma)^{16}\text{O}$ reaction rate (Woosley, Timmes & Weaver 1993; Thielemann, Nomoto & Hashimoto 1996; Arnett 1996). These stars develop CO cores of mass 0.6 and $1.0 M_{\odot}$. The central mass fractions are $X_{\text{C}} = 0.233, X_{\text{O}} = 0.739$ and $X_{\text{C}} = 0.316, X_{\text{O}} = 0.655$ respectively. In our unpublished calculations of the evolution of population I helium stars, using the Arnett (1996) reaction rate, we find slightly higher central oxygen abundances. In the context of dredge-up of oxygen diffusing from the core a more relevant quantity is the O mass fraction just below the extinct helium burning shell. The Salaris et al. (1997) models give $X_{\text{O}} \approx 0.02$ at the center of the helium shell. For the population I helium stars, we find $X_{\text{O}} \approx 0.05$ at the same location.

To get some idea of how the abundance of oxygen in the core affects the amount of oxygen dredged up to the surface, we have made two additional evolutionary sequences, P6LO3 and P6LO2 for $0.6 M_{\odot}$ cores of composition $X_{\text{C}} = 0.99, X_{\text{O}} = 0.01$. Although the abundance profiles in our white dwarf models differ in detail from those of the evolutionary calculations, the two values of core oxygen abundance considered here roughly bracket the possible range of oxygen abundance in the region below the helium shell. In figure 6, we show the O to He ratio as a function of T_{eff} for these two sequences and the P6HE2 and P6HE3 sequences. In the sequences with the thicker helium layer

Table 2. Properties of the convective zones for the coolest model of each HE sequence

| Sequence | T_{eff} | M_{conv} | T_{conv} | ρ_{conv} |
|----------|------------------|------------------------|-------------------|----------------------|
| P6HE6 | 9,930 | 1.973×10^{-7} | 3.08 | 33.7 |
| P6HE4 | 7,640 | 6.950×10^{-7} | 2.26 | 117 |
| P6HE3 | 6,830 | 7.015×10^{-6} | 1.07 | 740 |
| P6HE2 | 6,960 | 7.621×10^{-5} | 0.857 | 3610 |

Units are M_{\odot} for masses, K for T_{eff} , 10^6 K for T_{conv} , and 10^2 g cm $^{-3}$ for ρ_{conv} .

**Figure 4.** The solid lines are the values of $\log n(\text{C})/n(\text{He})$ for the P6HE6, P6HE4, P6HE3 and P6HE2 sequences. Also shown with error bars are the observed ratios.**Figure 5.** As figure 4 but for the 1HE4 and 1HE3 sequences.

very little oxygen is dredged to the surface, independent of the amount of oxygen in the core. For both of the thinner helium envelopes, oxygen is expected to be present in detectable amounts (based on a comparison of the oscillator strengths of the O I multiplets at 130.5 and 777.4 nm with the detected C I lines). Also the maximum photospheric oxygen abundance depends on the core oxygen abundance.

In the P6HE3 sequence with $X_{\text{O,core}} = 0.5$, the maximum photospheric abundance is $\log n(\text{O})/n(\text{He}) = -4.0$ which occurs at $T_{\text{eff}} = 8.0 \times 10^3$ K and in the P6LO3 sequence with $X_{\text{O,core}} = 0.01$, the maximum photospheric abundance is $\log n(\text{O})/n(\text{He}) = -5.3$ which occurs at $T_{\text{eff}} = 8.3 \times 10^3$ K. Hence measurement of the photospheric oxygen abundance in a DQ has the potential of providing useful information about the interior composition of the white dwarf.

3.3 The DBV GD 358

UV spectroscopy of the DBV GD 358 by Provencal et al. (1996) has confirmed the detection of He II 164.0 nm and C II 423.5 nm, first reported by Sion et al. (1988). Thus GD 358 can be considered to be the hottest DQ star, with $T_{\text{eff}} \approx 27,000$ K and $\log n(\text{C})/n(\text{He}) = -5.65 \pm 0.10$ (Provencal et al. 1996). At this temperature, the star is sufficiently old that heavy elements will have sunk deep beneath the photosphere yet too hot for a deep convection zone to develop and dredge-up carbon diffusing out of the core, unless the helium layer is very thin.

Dehner & Kawaler (1995) have investigated the possibility that GD 358 is a descendant of PG1159. They calculate the evolution of the abundance profiles in a star that has an initial envelope of mass $3 \times 10^{-3} M_{\odot}$ and composition 30% He, 35% C and 35% O by mass. When the star has cooled to the temperature range of the DBV's, they find that the star has a layer of pure helium of mass $10^{-5.5} M_{\odot}$, in good agreement with the asteroseismological analysis of the WET observations by Bradley & Winget (1994). Our P6PG6 sequence begins with a helium mass comparable to that found by asteroseismology for GD 358. When $T_{\text{eff}} = 27,000$ K, the center of the transition from He to C is at a mass depth of $10^{-6.7} M_{\odot}$, i.e. an order of magnitude less than found from asteroseismology, yet the photospheric $n(\text{C})/n(\text{He})$ is $\sim 10^{-20}$, which is many orders of magnitude smaller than observed. To get a detectable C to He ratio at 27,000 K, the helium layer mass cannot be too much larger than the convection zone, which at this temperature has its base at mass depth of $10^{-14} M_{\odot}$. Hence scenarios in which GD 358 is a descendant of the PG1159 star suffer from a conflict between the requirement that the helium layer mass be consistent with asteroseismology and the requirement that it be very small for C to be present in the photosphere at the observed abundance.

Other possible sources for the photospheric carbon are: 1) that it is radiatively supported, 2) accretion from the ISM and 3) that it is left over from a merger of two low mass white dwarfs in a double degenerate binary.

Detailed calculations of radiative levitation in helium

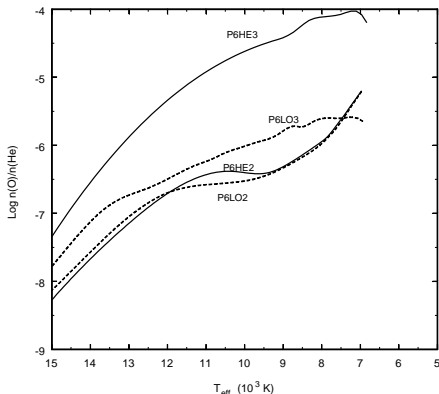


Figure 6. The values of $\log n(\text{O})/n(\text{He})$ for the P6HE3 and P6HE2 (solid lines) and the P6LO3 and P6LO2 (dashed lines) sequences.

dominated atmospheres have recently been presented by Chayer, Fontaine & Wesemael (1995), who find that, for $T_{\text{eff}} < 4 \times 10^4$ K, the radiatively levitated abundance of carbon is significantly less than $n(\text{C})/n(\text{He}) = 10^{-6}$. Hence radiative levitation appears to be insufficient to support carbon at the levels observed in GD 358.

Clearly, if accretion is invoked as the mechanism for the presence of photospheric carbon, then an explanation of why hydrogen has a low photospheric abundance of $n(\text{H})/n(\text{He}) \leq 3 \times 10^{-5}$ (Provencal et al. 1996) is needed. Mechanisms that prevent or inhibit accretion have been reviewed by Alcock & Illarionov (1980). However most of these mechanisms work equally well for carbon as for hydrogen. One mechanism that permits differential accretion is that the white dwarf has sufficiently high rotation rate and magnetic field that the ‘propeller’ mechanism (Illarionov & Sunyaev 1975) reduces the accretion rate of ionized hydrogen below the Bondi-Hoyle rate. A significant fraction of the carbon in the interstellar medium (ISM) can be in the form of grains, which have a significantly lower charge to mass ratio than protons so that they follow independent particle trajectories while outside the white dwarf’s magnetosphere (Alcock & Illarionov 1980). If they cross into the magnetosphere and are then evaporated by the radiation from the white dwarf, they provide a source of ionized carbon and other species that can then follow magnetic field lines to the white dwarf’s surface. The requirements for an effective propeller are discussed by Alcock & Illarionov (1980) and Stella, White & Rosner (1986). Accretion of ionized hydrogen is centrifugally inhibited if the co-rotation radius, r_c , is less than the magnetospheric radius, r_m . By studying multiplet splitting in their WET observations of the oscillations of GD 358, Winget et al. (1994) find evidence for a magnetic field of average strength 1300 ± 300 G and for differential rotation with the outer envelope rotating with a period of 0.89 d. With these parameters, $r_c \approx 5 \times 10^9$ cm. To determine r_m , we equate the magnetic energy density to the kinetic energy density on the symmetry axis of the (upstream) accretion flow. Assuming a dipole magnetic field of strength B_* ,

$$r_m = 8 \times 10^{10} \left(\frac{B_*}{10^3 \text{G}} \right)^{4/9} \left(\frac{R_*}{10^9 \text{cm}} \right)^{4/3} \left(\frac{v_\infty}{50 \text{km s}^{-1}} \right)^{2/9} n_\infty^{-2/9} \left(\frac{M_*}{M_\odot} \right)^{-1/3} \text{cm} \quad (13)$$

where v_∞ and n_∞ are the velocity of the ISM relative to the star and the ISM number density respectively. For GD 358, Provencal et al. (1996) find $v_\infty \approx 40$ km s $^{-1}$ and hence $r_m > r_c$ if $n_\infty < 3 \times 10^5$ cm $^{-3}$, which is the case for much of the volume of the ISM. Hence the propeller mechanism is capable of inhibiting accretion of ionized material by GD 358 and this may be the reason why the photospheric abundance of hydrogen is low. However, for carbon to be accreted at a greater rate than hydrogen, we also require that the characteristic distance at which incoming grains evaporate, r_e , be less than r_m . The temperature of dust grains of characteristic size $0.3 \mu\text{m}$ heated by the radiative flux from a star of distance r and luminosity L is (Osterbrock 1989)

$$T_d \approx 10^3 \left(\frac{L}{0.1 L_\odot} \right)^{1/5} \left(\frac{r}{10^{13} \text{cm}} \right)^{-2/5} \text{K} \quad (14)$$

For refractory grains which evaporate at $\approx 10^3$ K, $r_e \approx 10^{13}$ cm which is much greater than r_m for any values of n relevant to the ISM. Hence it is unlikely that the propeller mechanism can inhibit accretion of hydrogen without doing the same for carbon. From our P6PG6 sequence, we estimate that the time scale for settling of carbon out of the convection zone is about 0.1 yr. Hence, in a steady state, carbon has to be accreted at a rate of $4 \times 10^{-19} M_\odot \text{yr}^{-1}$ to maintain the observed photospheric abundance. For fluid dynamical accretion, and cosmic abundances this requires an ISM density of $n_{\text{H}} = 5$ cm $^{-3}$, which is higher than in the local ISM.

The merging of two white dwarfs in a double degenerate scenario is a complex process that is poorly understood. However it might reasonably be expected that the result of the merger is a luminous object that has much evolution to go through before reaching properties similar to those of GD 358. Hence given the short time scale for the evolution of the carbon distribution, it would be a remarkable coincidence that we find the star just at the time it looks like GD 358.

Hence none of these mechanisms can satisfactorily explain the observed photospheric abundances in a way that is consistent with the data from asteroseismology.

4 CONCLUSIONS AND DISCUSSION

Our main conclusion is that use of up-to-date opacities in modeling the evolution of DQ white dwarfs removes the discrepancy between estimates of the helium layer masses from the observed carbon abundances and the predictions of stellar evolution theory. In particular the bulk of the DQ white dwarfs can be interpreted as having mass $0.6 M_\odot$ and helium layer masses between 10^{-3} and $10^{-2} M_\odot$.

We suggest that DQ white dwarfs with exceptionally high atmospheric C abundances, such as G35-26, are of higher than average mass and those with no C or very low C have lower than average mass.

We also predict that oxygen will be present in DQ white dwarf atmospheres in detectable amounts if the helium layer mass is near the lower limit compatible with stellar evolution theory. Determination of the oxygen abundance has the potential of providing information on the profile of oxygen in the core and hence on the important $^{12}\text{C}(\alpha, \gamma)^{16}\text{O}$ reaction rate.

In contrast to P86, we do not find a drop in photospheric carbon abundance near $T_{\text{eff}} = 7,000$ K. Unfortunately, we are not able to continue our calculations below this temperature due to lack of opacity tables for low temperatures. Furthermore, for T_{eff} below about 10,000 K, uncertainties in the equation of state are becoming increasingly important. In particular, the equation of state is becoming sensitive to the treatment of Stark ionization. Hence we do not rule out the possibility that partial recombination of carbon occurs below the convection zone leading to a drop in photospheric carbon abundance as found by P86.

ACKNOWLEDGMENTS

JM thanks Judi Provencal for useful discussions and the Human Capital and mobility programme (CHGE-CT92-0009) "Access to Supercomputing Facilities", established between the EC and the CESCA/CEPBA. MH thanks the CIRIT for a grant to visit the University of Delaware, as well as the Department of Physics & Astronomy of the University of Delaware for hospitality during her stay. We also thank partial support from the DGICYT Projects PB94-0111 and PB94-0827-C02-02.

REFERENCES

- Alcock C., Illarionov A., 1980, ApJ, 235, 541
 Aller L.H., Chapman S., 1960, ApJ, 132, 461
 Arnett D., 1996, *Supernovae and Nucleosynthesis*. Princeton University Press, Princeton, NJ, p. 228
 Bradley P.A., Winget D.E., 1994, ApJ, 421, 236
 Burgers J.M., 1969, *Flow Equations for Composite Gases*. Academic, New York
 Chayer P., Fontaine G., Wesemael F., 1995, ApJS, 99, 189
 Curtiss C.F., Hirschfelder J.O., 1949, J. Chem. Phys., 17, 550
 D'Antona F., Mazzitelli I., 1991, in Michaud, G., Tutukov, A., eds, Proc. IAU Symp. 145, *Evolution of Stars: The Photospheric Abundance Connection*. Kluwer, Dordrecht, p. 399
 Dehner B.T., Kawaler S.D., 1995, ApJ, 445, L141
 Domínguez I., Tornambé A., Isern J., 1993, ApJ, 419, 268
 Fontaine G., Michaud G., 1979, ApJ, 231, 826
 Fontaine G., Graboske H.C., Van Horn H.M., 1977, ApJS, 35, 293
 Fontaine G., Tassoul M., Wesemael F., 1984, in Noels A., Gabriel M., eds, Proc. 25th Liège Astrophysical Coll., *Theoretical Problems in Stellar Stability and Oscillation*. Université de Liège, Liège, p. 328
 Huebner W.F., Merts A.L., Magee N.H., Argo M.F., 1977, Los Alamos Scientific Report LA-6760-M
 Hummer D.G., Mihalas D., 1988, ApJ, 331, 794
 Iben I., Jr., 1984, ApJ, 277, 333
 Iben I., Jr., MacDonald J., 1985, ApJ, 296, 540
 Iben I., Jr., Tutukov A., 1984, ApJ, 282, 615
 Iben I., Jr., Tutukov A., 1996, ApJS, 105, 145
 Iglesias C.A., Rogers F.J., 1993, ApJ, 412, 752
 Illarionov A., Sunyaev R., 1975, A&A, 39, 185
 Muchmore D., 1984, ApJ, 278, 769
 Osterbrock D.E., 1989, *Astrophysics of Gaseous Nebulae and Active Galactic Nuclei*. University Science Books, Mill Valley, CA, p. 227
 Paquette C., Pelletier C., Fontaine G., Michaud G., 1986a, ApJS, 61, 177
 Paquette C., Pelletier C., Fontaine G., Michaud G., 1986b, ApJS, 61, 197
 Pelletier C., Fontaine G., Wesemael F., Michaud G., Wegner, G., 1986, ApJ, 307, 242 (P86)
 Provencal J.L., Shipman H.L., Thejll P., Vennes S., Bradley P.A., 1996, ApJ, 466, 1011
 Ritossa C., García-Berro E., Iben I., Jr., 1996, ApJ, 460, 489
 Salaris M., Domínguez I., García-Berro E., Hernanz M., Isern J., Mochkovitch R., 1997, ApJ, in press
 Sion E.M., Liebert J., Vauclair G., Wegner G., 1988, in Wegner G., ed., Proc. IAU Coll. 114, *White Dwarfs*. Springer-Verlag, New York, p. 354
 Stella L., White N.E., Rosner R., 1986, ApJ, 308, 669
 Thejll P., Shipman H.L., MacDonald J., MacFarland W., 1990, ApJ, 361, 197
 Thielemann F.-K., Nomoto K., Hashimoto M., 1996, ApJ, 460, 408
 Vassiliadis E., Wood P.R., 1993, ApJ, 413, 641
 Vauclair G., Vauclair S., Greenstein J., 1979, A&A, 80, 79
 Weaver T.A., Woosley S.E., 1993, Phys. Rep., 227, 65
 Weidemann V., Koester D., 1995, A&A 297, 216
 Winget, D.E. et al., 1994, ApJ, 430, 839
 Woosley S.E., Timmes F.X., Weaver T.A., 1993, in Käppeler F., Wisshak K., eds, *Nuclei in the Cosmos*. IOP Publishing Ltd, London, p. 531

This paper has been produced using the Royal Astronomical Society/Blackwell Science \TeX macros.